Journal of Power Sources 251 (2014) 8–13

Contents lists available at ScienceDirect

Journal of Power Sources

journal homepage: www.elsevier.com/locate/jpowsour

Thermophysical properties of $LiFePO_4$ cathodes with carbonized pitch coatings and organic binders: Experiments and first-principles modeling

Jagjit Nanda [a,*,2], Surendra K. Martha [a,1], Wallace D. Porter [a], Hsin Wang [a], Nancy J. Dudney [a,**], Maxwell D. Radin [b], Donald J. Siegel [c,d]

[a] Materials Science and Technology Division, Oak Ridge National Laboratory, Oak Ridge, TN 37831, USA
[b] Department of Physics, University of Michigan, Ann Arbor, MI 48109, USA
[c] Mechanical Engineering Department, University of Michigan, Ann Arbor, MI 48109, USA
[d] Applied Physics Program, University of Michigan, Ann Arbor, MI 48109, USA

HIGHLIGHTS

- Experimental heat capacity of $LiFePO_4$ agrees well with first principle calculation.
- Thermal diffusivity of carbon pitch coated $LiFePO_4$ is factor of two higher.
- $LiFePO_4$–carbon–binder electrode compositions have lower thermal diffusivity.
- Binder and carbon coated $LiFePO_4$ have similar thermal reactivity in electrolyte.

ARTICLE INFO

Article history:
Received 9 August 2013
Received in revised form
14 October 2013
Accepted 11 November 2013
Available online 19 November 2013

Keywords:
Lithium battery
Battery electrodes
Thermophysical properties
Heat capacity
Density functional theory
Lithium iron phosphate

ABSTRACT

We report heat capacity, thermogravimetry and thermal diffusivity data for carbonized mesophase pitch coated $LiFePO_4$ (LFP) cathodes. The results are compared with the thermophysical properties of a conventional LFP-based electrode having a poly (vinylene) difluoride (PVDF) binder and conductive carbon diluents. The measured heat capacity of LFP as a function of temperature is in good agreement with model calculations based on first-principles methods. Thermal diffusivity data indicate that the mesophase pitch coated LFP compositions have a factor of two higher thermal diffusivity than the conventional electrode composition, suggesting that the coatings improve heat transfer. In the presence of an electrolyte mixture (1.2 M lithium hexa-fluorophosphate), differential scanning calorimetry (DSC) analysis of the LFP–pitch composite and LFP–PVDF–carbon composites showed similar onset temperature and heat evolution.

© 2013 Published by Elsevier B.V.

1. Introduction

Increases in the capacity of modern lithium (Li) batteries continue to be made possible by improvements in the electronic conductivities and ionic diffusivities of the anode and cathode materials [1]. $LiFePO_4$ (LFP) is a promising and well-known cathode material for high-power rechargeable lithium-ion batteries [2]. At present, the primary flaws of LFP that limit its application are low electronic conductivity and slow lithium diffusion [2,3]. Consequently, several approaches are being explored to improve its transport properties [2,3]. For example, the use of nanoparticles as the active material improves kinetics due to the reduction in diffusion length for ionic transport; furthermore, the relatively high surface area of the nanoparticulate morphology promotes fast interfacial charge transfer. Common approaches to address the inherently low electronic conductivity of LFP include [2,3] the addition of conducting diluents such as graphitic carbon or fibers, and/or coating the surface of LFP powders with a thin amorphous

* Corresponding author. Tel.: +1 865 241 8361.
** Corresponding author.
E-mail addresses: nandaj@ornl.gov, nandaj@gmail.com (J. Nanda), dudneynj@ornl.gov (N.J. Dudney).
[1] Present address: Department of Chemistry, Indian Institute of Technology Hyderabad, Ordnance Factory Estate, Yeddumailaram 502205, AP, India.
[2] Also at Department of Chemical & Biomolecular Engineering, University of Tennessee, Knoxville, TN 37996, USA.

0378-7753/$ – see front matter © 2013 Published by Elsevier B.V.
http://dx.doi.org/10.1016/j.jpowsour.2013.11.022

carbon layer. These approaches significantly improve the electronic conductivity between particles and also improve capacity retention.

Our recent research on petroleum pitch (P-pitch) coated carbon grids has demonstrated another pathway for improving the performance of LFP-based batteries. These materials can potentially replace Al foil current collectors in lithium batteries, without compromising electrochemical performance [4,5]. In this approach, a slurry composition of mesophase pitch and LFP particles is coated on micron sized (diameter) graphitic carbon fiber mats and carbonized to 700 °C under argon atmosphere. This process allows for free-standing electrodes that do not require a metal current collector or polymeric binders, resulting in further increases to the energy density of the electrodes. The carbon fibers exhibit a range of thermal and electrical conductivities, some even comparable to current collectors such as aluminum [6]. In addition, the electrochemical performance of carbon fiber based mats and individual carbon fiber coated electrodes showed excellent capacity retention and rate capability, providing a practical route toward fiber based electrode architectures. [4] Specifically, using Toray carbon fiber paper derived from poly-acrylonitrile (PAN) based precursor and Pyrograf-1 carbon fiber mats as current collectors the P-pitch coated LFP electrodes demonstrated capacities exceeding to 160 mAh g^{-1} between C/20-2C current rate. Further, the cycle life performance of these electrodes compared well with the conventional electrodes (Al current collector) with similar active materials loading [4,5]. The electrochemical impedance spectroscopy (EIS) study of only carbon fiber electrodes and the annealed P-pitch coated electrodes clearly showed that the presence of carbonized P-pitch makes good electronic contact along and between the fibers.

In addition to revealing transport properties, understanding the thermophysical properties of electrical energy storage materials is important because thermal stability directly influences safety during continuous charge–discharge cycling. [1,7–9]. These issues are paramount for lithium-ion chemistries where lithium plating, over potential, and potential exothermic reactions [10,11] between charged electrodes, electrolytes and other cell components can lead to safety concerns [12]. In this study we report thermophysical properties of conventional LFP electrode compositions and compare them with their P-pitch coated LFP counterparts. The first part of our analysis discusses heat capacity and thermogravimetric analysis (TGA) of components of the electrodes, including mesophase pitch, LFP, and binder–LFP mixtures. The results are then discussed in the context of the thermal diffusivity behavior of composite electrodes. Specifically, we compare the thermal diffusivity of the LFP-carbonized pitch composition with a commercial electrode composition comprised of LFP, polyvinylidene fluoride (PVDF) binder, and conductive carbon diluents. Further, we report experimental heat capacity values of LFP as a function of temperature and compare with heat capacity values from density functional theory (DFT) calculations. We find that the mesophase pitch coated LFP compositions exhibit a factor of two increase in thermal diffusivity compared to the conventional electrode composition, implying better heat transfer properties.

2. Methods: experimental and computational

Carbon coated $LiFePO_4$ (LFP) powders (3 wt.% carbon) were obtained from Hydro-Québec, Canada and pure LFP was provided by MTI Corporation, USA. The MTI LFP powders were carbon-free and were used as received. The particle size of both the LFPs was in the range 100–150 nm. Because of the air sensitivity of LFP, all samples were handled and stored under argon/vacuum atmosphere. Thermophysical measurements such as TGA, heat capacity and thermal diffusivity studies were carried out on pressed pellets. Slurries of LFP, PVDF, and C-black at desired compositions were prepared in N-vinylpyrrolidone (NVP) and dried at 80 °C. The powders were pressed into 1.27 cm diameter pellets with a pressure of 10 Ton for 2 min. The LFP and Pitch slurries were prepared with 95:5 wt.% compositions in NVP and dried at 80 °C followed by pressing with the above protocol. The pitch and LFP pellets were heated at 700 °C under Ar atmosphere for 5 h to carbonize the petroleum pitch. For TGA measurement the pellet dimensions were 4 mm in diameter and 1 mm thick. For thermal diffusivity measurements the pellet diameter was 1.27 cm with a thickness between 0.3 and 0.4 mm (for better accuracy, thin samples are preferred). Transmission electron microscopy (TEM) study reveals a uniform carbonaceous coating around LFP particles in the range of 5–10 nm. The degree of carbonization of P-pitch depends on the annealing temperature. In the work reported here it was about 700 °C. Raman spectroscopic study of the annealed P-pitch electrodes showed both disorder carbon peak (D band) at around 1350 cm^{-1} and the graphitic peak at 1590 cm^{-1} (G-band) implying we have mixed sp^2 and sp^3 binding environment. This was reported by us in an earlier publication [13].

Thermogravimetric analyses (TGA) of samples were carried out using a Stanton Redcroft TGA instrument (model STA 1500) under argon atmosphere. For this purpose, samples were loaded in platinum crucibles and the data were collected at 10 °C min^{-1} between 25 and 800 °C upon an Ar gas flow at 50 cc min^{-1}.

An Anter FL5000 laser flash system was used to obtain thermal diffusivity of the specimen. The system uses an Nd–Yag laser to deposit a short heat pulse on the sample surface and an InSb IR detector to record the back surface temperature rise. Thermal diffusivity was obtained using the ASTM 1461 flash diffusivity setup. Diffusivity measurements were carried out from 25 °C to 500 °C in a graphite furnace with 50 °C increments. The testing was performed under flowing Ar. In this technique the sample pellet is heated using a temperature-controlled furnace. The system is equipped with a six-sample carousel. Once the temperature is stabilized to the desired value, the laser is fired at the front face of the sample. The heat pulse due to the incident laser energy travels through the thickness of the sample and the temperature at the back surface is monitored using an infra-red detector. Three measurements were performed at each set point. The diffusivity values are calculated based on the sample thickness and temperature rise curve based on the Clark and Taylor method [14].

Differential scanning calorimetry (DSC) experiments were performed using NETZSCH DSC 404C calorimeter. The heating rate used was 20° min^{-1}. For DSC measurements the electrode and electrolyte were hermetically sealed in stainless steel pressure pans sealed with a gold gasket using a torque driver. The ratio of electrode material to electrolyte was about 1:2 wt./wt.

The theoretical heat capacity of LFP was calculated using density functional theory (DFT) within the PBE GGA [15] as implemented in the VASP code [16–19]. The simplified on-site Coulomb interaction U of Dudarev et al. [20] was used, with $U = 3.71$ eV for $LiFePO_4$ and 4.90 eV for $FePO_4$, as calculated from linear response theory by Zhou et al. [21]. The projector augmented wave method [22,23] was used with a 0.1 eV Gaussian smearing of electronic occupancies, and an antiferromagnetic magnetic ordering was assumed. The lattice constants were optimized on a conventional unit cell with a $12 \times 12 \times 12$ Monkhorst–Pack mesh [24] and a 600 eV planewave cutoff, and found to be 10.42, 6.06, and 4.74 Å; this compares well with the experimentally reported values of 10.33, 6.01, and 4.69 Å [25]. The same parameters were used for heterosite $FePO_4$ (heterosite $FePO_4$ is the delithiated form of $LiFePO_4$), whose lattice constants were found to be 9.92, 5.86, and 4.85 Å, in good agreement with the experimentally reported values of 9.76, 5.75, 4.76 Å [26].

The heat capacity was calculated within the harmonic approximation [27]:

$$C_v = \frac{1}{M}\sum_i \frac{\partial}{\partial T}\frac{\hbar\omega_i}{e^{\hbar\omega_i/k_BT}-1}.$$

The vibrational frequencies ω_i were determined using finite-differences to compute the dynamical matrix in a 1 × 2 × 2 supercell of mass M (112 atoms for $LiFePO_4$ and 96 atoms for $FePO_4$) with a 2 × 2 × 2 Monkhorst–Pack k-point mesh and a 400 eV planewave cutoff. We assume the volume to be independent of temperature (*i.e.* $C_p = C_v$).

3. Results and discussion

Thermophysical characterization of the individual electrode components such as the mesophase carbon pitch, LFP and LFP–binder, was undertaken first (Figs. 1 and 2). These experimental values were then used as an input for calculating the heat transfer properties such as thermal conductivity (K). As reported by Klett et al. the mesophase pitch undergoes a carbonization process to form an electrically conducting coating around the LFP at approximately 700 °C. Interestingly enough, when heat treated alone under argon atmosphere the pitch transforms into a porous, foam-like structure as shown in Fig 1(a). Fig. 1(b, c) shows the TGA and Fig. 1(d) heat capacity results for the mesophase P-pitch sample. Experiments on three sets of pitch sample were carried out in order to ascertain the accuracy of the measurements. Mesophase pitch precursors soften and then form a low density foam as gases are released [28]. The carbonization occurs between ~400 and 600 °C

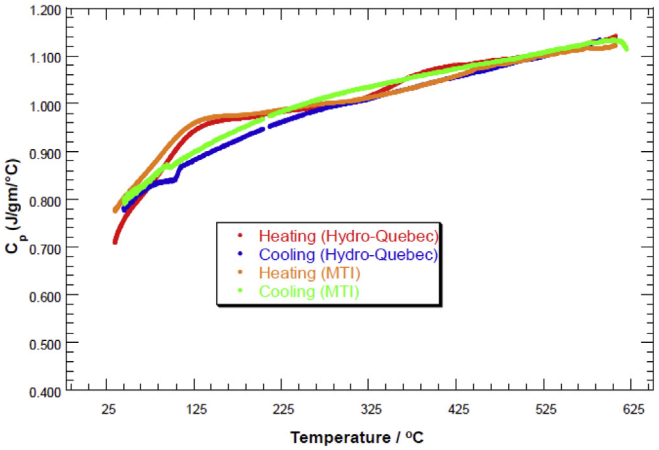

Fig. 2. Heat capacity versus temperature (between 25 and 600 °C) of $LiFePO_4$ obtained from two suppliers, Hydro-Québec and MTI respectively. Data are shown for both heating and cooling cycle. The sample from Hydro-Québec has between 2 and 3 wt.% carbon content.

as shown in Fig. 1(b, c), and is conductive even with a relatively low temperature treatment. However, the crystallinity and electronic, thermal transport continue to improve with higher temperature treatments. The heat flow peak showed an endothermic peak centered around 600 °C with an onset beginning close to 350 °C (Fig. 1(b, c)). The noise or peaks in the range of 350–450 °C arise mostly because of the evolution of gaseous by-products (hydrocarbons) as the pitch undergoes heating. The beginning mesophase

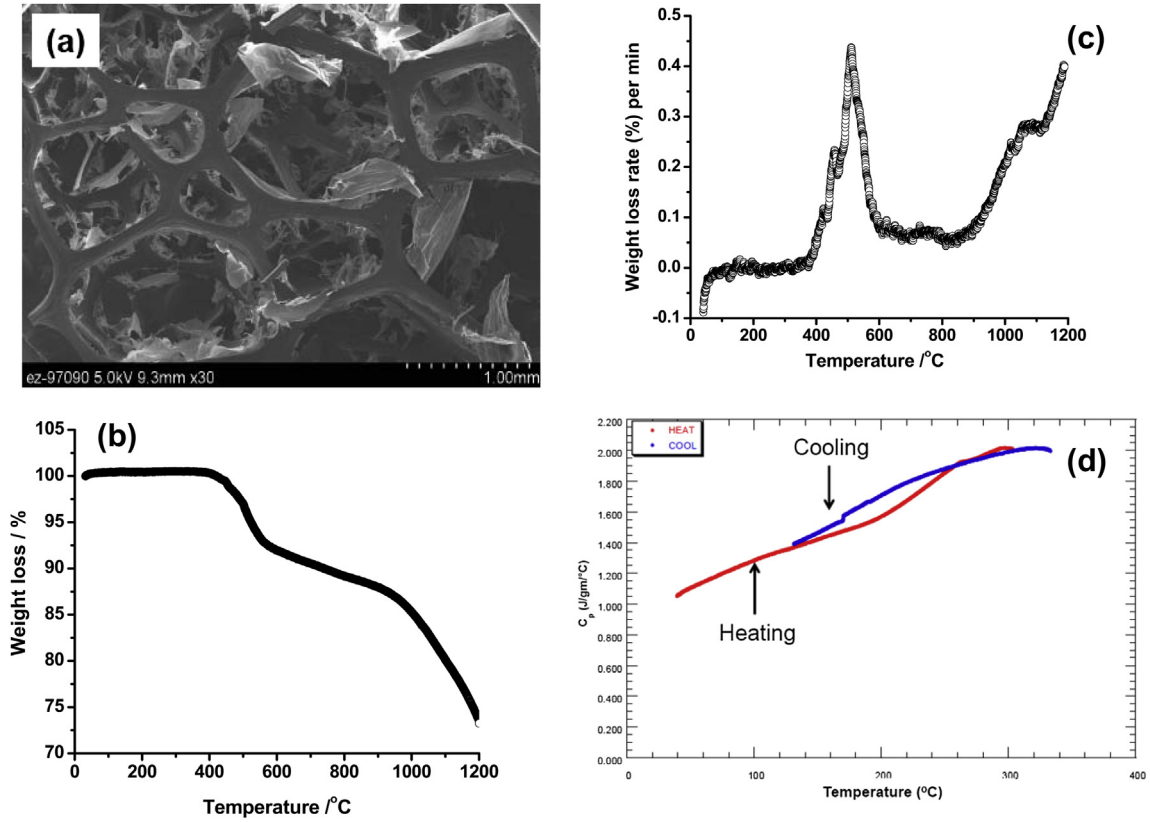

Fig. 1. (a) SEM image of P-pitch annealed at 700 °C indicating open-cell foam or honey comb structures. (b) TGA data of pure P-pitch upon heating at 10 °C min^{-1} under argon atmosphere between 25 and 700–1200 °C. (c) Heat flow versus weight loss in milligram during TGA under argon atmosphere between 25 and 700–1200 °C. (d) Heat capacity versus temperature result for P-pitch between 25 and 350 °C. Data are shown for heating (red) and cooling (blue) cycle. (For interpretation of the references to colour in this figure legend, the reader is referred to the web version of this article.)

pitch has a liquid crystalline phase that undergoes a pseudo order phase transition peaking at above 500 °C, similar to that observed in polymeric materials at the glass transition temperature. [29] This foaming process continues until the temperature climbs above 600 °C. The heat flow result closely correlates with the weight loss behavior of the mesophase pitch shown in Fig. 1(c). The weight loss rate slows as the temperature climbs above 700 °C, consistent with the heat flow data. From the TGA data we observe a net 17% weight loss (Fig. 1(b)) upon heating due to the slow decomposition of the hydrocarbon residues yielding partially graphitized domains. The pitch losses about 27% of its initial mass if heated to higher temperatures of 1200 °C.

3.1. Heat capacity

The variation in specific heat capacity of mesophase carbon pitch versus temperature is shown in Fig. 1(d). Based on the heat flow data we limit the heat capacity measurement to 350 °C, above which the mesophase pitch undergoes gas evolution and foaming. The heating and cooling curves are shown in Fig. 1(d). The heating data shows a small depression near 200 °C which is not present during the cooling cycle. This could be caused by decomposition of low melting point hydrocarbon derivatives present in the mesophase pitch.

The heat capacity data for the pure phase of LFP (MTI Corp., USA) and carbon coated LFP (2–3 wt.% carbon, Hydro-Québec, Canada) are compared in Fig. 2. The measurement was performed in the range of 25–600 °C under an argon atmosphere. We observe hysteresis between the heating and cooling data due to evolution of extrinsic materials in LFP like moisture and impurities. These processes appear as an endothermic peak in the heating curve, and are absent during the cooling cycle. The behavior of the heat capacity data versus temperature for both LFP samples shows similar trends and the experimental values are within the experimental accuracy of the measurement (about 2%).

Fig. 3 compares the heat capacity (C_p) results of pure phase LFP, pitch-coated LFP, and LFP–carbon–binder composites. Since the PVDF melting temperature is approximately 165 °C, we limit the heat capacity measurement to 150 °C for the binder phases. The pure LFP and the pitch-coated LFP have similar heat capacity values since addition of an extra few percent carbon does not affect the heat capacity values appreciably. Since the carbonized pitch is only <3 wt.% of the total composition it will not appreciably contribute to the heat capacity values across this temperature range. The binder compositions tend to have a higher heat capacity compared to pure LFP as one approaches higher temperature. This is explained by the presence of lower atomic weight elements such as hydrogen, carbon and fluorine in PVDF. The nominal binder amount used during this measurement was 7.5 and 10 wt.%. The experimental heat capacity values for pure phase LFP varies between 0.4 and 1.05 J g^{-1} °C^{-1} between the measured temperature ranges of −140–500 °C. There appears to be a parabolic dependence of C_p with respect to temperature. The C_p increases with T to until 300–350 °C and remains steady after that.

In order to investigate further we compare the calculated and experimental heat capacity of LFP as a function of temperature as reported in Fig. 4. Overall, the calculated specific heat is in very good agreement with the experimental data: at temperatures below 300 °C the calculated values overestimate those from experiment by at most 8%. We note that our assumption of fixed volume in the calculation cannot explain this minor discrepancy, because C_p in general is larger than C_v [30]. The small bump in the experimental data at about 400 °C could be due to the presence of impurities or a non-stoichiometry in the sample. To examine the latter possibility, we have calculated the heat capacity assuming a two-phase mixture of 70 mol % $LiFePO_4$ and 30 mol % heterosite $FePO_4$ (heat capacities obtained using the lower energy rodolicoite $FePO_4$ structure are similar). As can be seen in Fig. 4, this two-phase model shows slightly better agreement with the experimental data below 300 °C. ($FePO_4$ has a somewhat lower heat capacity than $LiFePO_4$ due to the removal of the lighter weight lithium atoms.) We note that the Li_xFePO_4 system is known to undergo a phase transition from a two-phase region to a disordered state; at a composition of $x = 0.7$, this transition has been experimentally observed to occur at a temperature of approximately 200–250 °C [31,32]. Such a transition could also explain the variation between theory and experiment at higher temperatures. Of course, the evolution of extrinsic species, such as moisture, could also be a factor.

3.2. Thermal diffusivity

Fig. 5 shows the thermal diffusivity (D) versus temperature for both pitch-coated and binder based LFP compositions. Through plane diffusivity measurements were performed using the laser flash method. In the case of the pitch–LFP mixture the diffusivity measurements were performed at temperatures up to 500 °C,

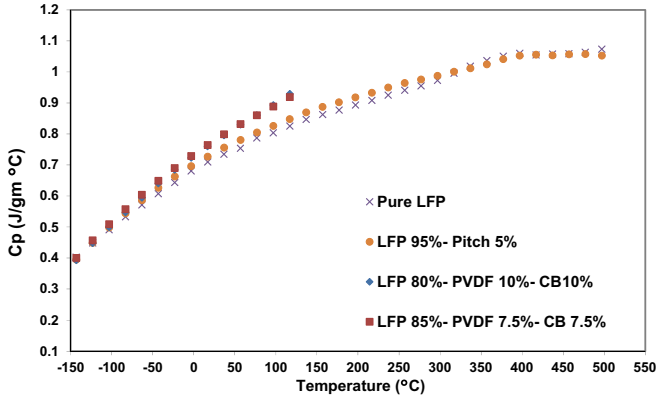

Fig. 3. Heat capacity versus temperature of $LiFePO_4$ (cross) from Hydro-Québec, $LiFePO_4$ + pitch (solid circle) and $LiFePO_4$ + PVDF + carbon black (solid squares and diamond). The binder compositions are limited to 120 °C due to the low melting point of PVDF.

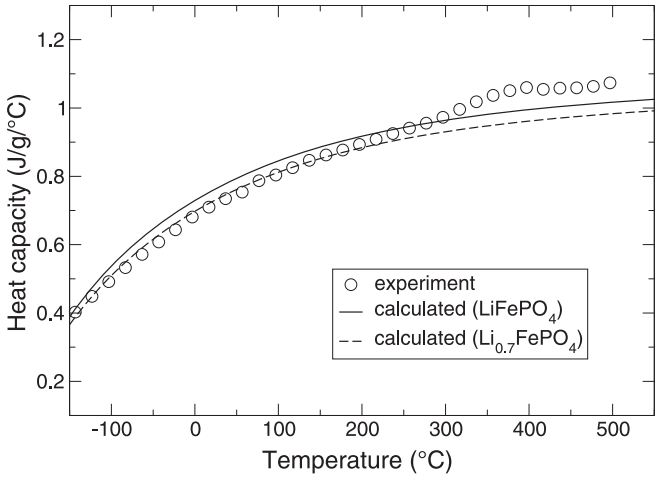

Fig. 4. Calculated heat capacity using DFT and comparison with experimental data for Hydro-Québec LFP as a function of temperature. Solid line shows the calculated heat capacity of pure $LiFePO_4$, while the dashed line shows that of a two-phase mixture of 70 mol % $LiFePO_4$ and 30 mol % $FePO_4$.

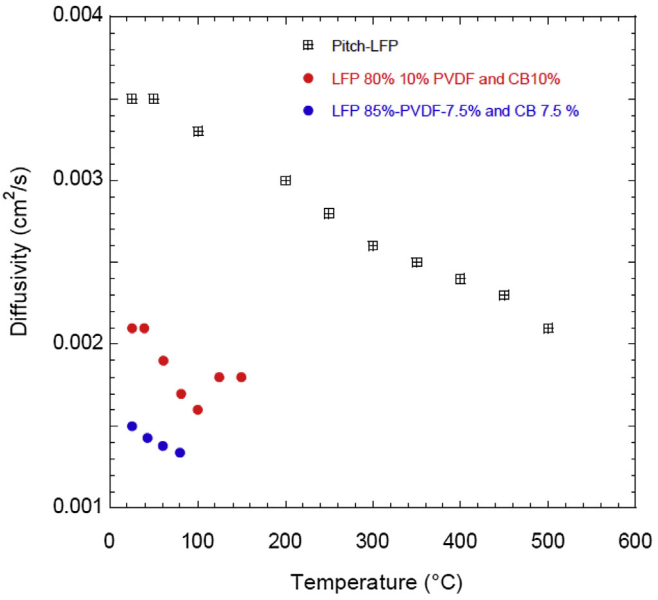

Fig. 5. Thermal diffusivity versus temperature of $LiFePO_4$ + pitch (box) and 10 and 7.5 wt.% PVDF composition (red and blue circles). (For interpretation of the references to colour in this figure legend, the reader is referred to the web version of this article.)

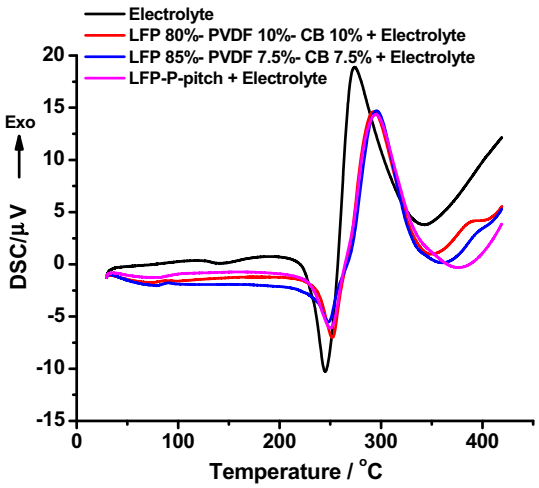

Fig. 6. DSC result of LFP electrode compositions with electrolyte mixture (1.2 M $LiPF_6$ + EC + DMC). Black line: electrolyte mixture only. Blue line: LFP electrode composition, 80% LFP + 10% C-black + 10% PVDF. Green line 85% LFP + 7.5% C-black + 7.5% PVDF. Red line: LFP + 5 wt.% coated pitch only. (For interpretation of the references to colour in this figure legend, the reader is referred to the web version of this article.)

while for the binder compositions we limit the measurements to between 120 and 140 °C to avoid any thermal decomposition. Thermal diffusivity values for all compositions showed a linear decrease with increasing temperature within the measured range. The diffusivity plot for the 10% binder composition shows two data points measured at 125 and 150 °C, respectively, which is close to the temperature where PVDF begins to melt. The jump in the values could be a manifestation of this effect. Therefore, diffusivity was measured only up to 100 °C for the 7.5% binder composition.

Several interesting observations can be made from the thermal diffusivity measurements at different temperatures for the LFP electrode compositions. The temperature dependence of diffusivity for all cases seems to be linear and falls with increasing *T*. This is expected since diffusivity values drop due to an increased phonon scattering rate at higher temperature. [33] The binder (PVDF) LFP has approximately a factor of two lower diffusivity compared to the pitch coated samples, implying that PVDF–CB has lower thermal transport compared to carbonized pitch. For example, as illustrated in Fig. 6 at 100 °C one of the LFP–PVDF–CB compositions *D* was in the order of 0.0016 $cm^2\ S^{-1}$ the corresponding value for the LFP–pitch was 0.0032 $cm^2\ S^{-1}$.

Between the two PVDF–CB compositions we notice higher diffusivity for the composition that has higher PVDF content (10 wt.%). This is could be mostly due to higher carbon black content (10 versus 7.5 wt.%) and a relatively lower LFP content (80% instead of 85%).

From the experimentally measured values of heat capacity, thermal diffusivity and densities we can estimate the thermal conductivity (*K*) for each compositions using the relation $K = \rho C_p D$; where ρ is the density, C_p is the heat capacity and *D* is thermal diffusivity. The density values of the pellets were estimated from their respective weights and dimensions. Table 1 summarizes the comparison between the thermal conductivity values at 25 °C of pitch–LFP and the LFP–binder compositions. From Table 1 it is clear that LFP–pitch compositions exhibit a factor of 2 increase in thermal conductivity compared to the conventional LFP–binder (PVDF) plus conductive diluents (CB) electrode. This signifies that heat transfer across pitch–LFP materials occurs at a higher rate than across LFP–PVDF–CB composite materials.

3.2.1. DSC study of pitch coated LFP

Fig. 6 shows DSC data for various LFP compositions in the presence of an electrolyte consisting of 1.2 M $LiPF_6$ in 1:2 wt./wt. proportion to an Ethylene Carbonate (EC)–Dimethyl Carbonate (DMC) mixture. The ratio between the active electrode material and electrolyte was 1:2 wt./wt. DSC analysis of carbonate solvents with and without $LiPF_6$ salt has been reported by several groups [10,34]. The intensity, onset temperature, and peaks of the various endothermic and exothermic features in DSC depend on variety of factors such as, heating rate, reactivity between individual components of the mixture and relative concentration of solvents or molar ratios. [10] The goal of the present study is to compare the reactivity of a standard electrolyte mixture (1.2 M $LiPF_6$) with pitch-coated LFP to that of a standard LFP–binder–CB composite. The heat of reaction curve for the electrolyte by itself is shown by the solid black line of Fig. 6. The data indicates an endothermic peak around 240 °C (most likely arising from the $LiPF_6$), followed by a relatively large exothermic peak from EC–DMC decomposition. Compared to the pure electrolyte, the DSC peak for samples containing both the electrode and electrolyte is reduced in intensity, most likely due to lower carbonate concentration. Also the peak onset is moved toward slightly higher temperatures. From the DSC results it appears that the heat of reaction for LFP–Pitch and the LFP–PVDF–CB composition are similar for this particular electrolyte mixture with only subtle differences at higher temperatures (>300 °C).

4. Conclusion

We report a comprehensive set of thermophysical measurements for Li-ion cathode materials comprised of pure LFP, mesophase pitch coated LFP, and “conventional” compositions based on LFP–binder–carbon diluents. Thermal Diffusivity results reveal that pitch-coated LFP has approximately a factor of two higher diffusivity compared to LFP–binder compositions. The experimental LFP heat capacity values agree very well with models based on DFT calculations. Temperature dependent diffusivity measurement over the region of interest showed a linear dependence for LFP–pitch as well as binder compositions. Based on the experimentally measured thermophysical properties we calculate the

Table 1
Room temperature thermal conductivity (K) values calculated from thermophysical measurements at 25 °C.

Sample Description	wt.% $LiFePO_4$	wt.% carbon	wt.% PVDF	Measured density (ρ) (g cc^{-1})	Measured heat capacity (C_p) (J g^{-1} °C)	Measured thermal diffusivity (cm^2 s^{-1})	Calculated thermal conductivity (W m^{-1}-K) $K = \rho C_p D$
$LiFePO_4$–Pitch-annealed at 700 °C	95	5	0	2.06	0.741	0.0035	0.53
$LiFePO_4$ 80%–CB 10%–PVDF 10%	80	10	10	1.65	0.778	0.0021	0.27
$LiFePO_4$ 85% –PVDF 7.5%–CB 7.5%	85	7.5	7.5	2.31	0.778	0.0015	0.27

thermal conductivity values for each of these compositions. Furthermore DSC results demonstrate that the thermal reactivity behavior of pitch and binder based LFP composition are similar with respect to $LiPF_6$–carbonate mixtures. Our result shows that pitch based LFP carbon fiber electrodes can provide better heat conduction properties compared to the conventional binder based aluminum electrodes. We anticipate that this approach can also be applied to other high capacity electrode materials used in lithium-ion batteries.

Acknowledgments

The authors thank Karim Zaghib of Hydro-Québec for supplying the $LiFePO_4$ powders used in this study. This work is supported by the Assistant Secretary for Energy Efficiency and Renewable Energy, Office of Vehicle Technologies of the U.S. Department of Energy. Part of the work was also supported under High Temperature Materials User program funded by Office of Vehicle Technology, EERE Department of Energy. M.D.R. and D.J.S acknowledge financial support from U.S. Department of Energy's U.S.-China Clean Energy Research Center – Clean Vehicles Consortium (CERC-CVC), Grant DE-PI0000012.

References

[1] M. Park, X. Zhang, M. Chung, G.B. Less, A.M. Sastry, J. Power Sources 195 (2010) 7904–7929.
[2] L.-X. Yuan, Z.-H. Wang, W.-X. Zhang, X.-L. Hu, J.-T. Chen, Y.-H. Huang, J.B. Goodenough, Energy Environ. Sci. 4 (2011) 269–284.
[3] M. Gaberscek, R. Dominko, J. Jamnik, Electrochem. Commun. 9 (2007) 2778–2783.
[4] S.K. Martha, J.O. Kiggans, J. Nanda, N.J. Dudney, J. Electrochem. Soc. 158 (2011) A1060–A1066.
[5] A.K. Kercher, J.O. Kiggans, N.J. Dudney, J. Electrochem. Soc. 157 (2010) A1323–A1327.
[6] J.F. Snyder, E.L. Wong, C.W. Hubbard, J. Electrochem. Soc. 156 (2009) A215–A224.
[7] M.M. Farid, A.M. Khudhair, S.A.K. Razack, S. Al-Hallaj, Energy Convers. Manag. 45 (2004) 1597–1615.
[8] A. Sharma, V.V. Tyagi, C.R. Chen, D. Buddhi, Renew. Sustain. Energy Rev. 13 (2009) 318–345.
[9] L. Wang, F. Zhou, Y.S. Meng, G. Ceder, Phys. Rev. B 76 (2007) 165435.
[10] G.G. Botte, R.E. White, Z. Zhang, J. Power Sources 97–98 (2001) 570–575.
[11] N. Katayama, T. Kawamura, Y. Baba, J.-i. Yamaki, J. Power Sources 109 (2002) 321–326.
[12] M.S. Islam, D.J. Driscoll, C.A.J. Fisher, P.R. Slater, Chem. Mater. 17 (2005) 5085–5092.
[13] S.K. Martha, N.J. Dudney, J.O. Kiggans, J. Nanda, J. Electrochem. Soc. 159 (2012) A1652–A1658.
[14] L.M. Clark III, R.E. Taylor, J. Appl. Phys. 46 (1975) 714–719.
[15] J.P. Perdew, K. Burke, M. Ernzerhof, Phys. Rev. Lett. 77 (1996) 3865–3868.
[16] G. Kresse, J. Hafner, Phys. Rev. B 47 (1993) 558–561.
[17] G. Kresse, J. Hafner, Phys. Rev. B 49 (1994) 14251–14269.
[18] G. Kresse, J. Furthmuller, Phys. Rev. B 54 (1996) 11169–11186.
[19] G. Kresse, J. Furthmüller, Comput. Mater. Sci. 6 (1996) 15–50.
[20] S.L. Dudarev, G.A. Botton, S.Y. Savrasov, C.J. Humphreys, A.P. Sutton, Phys. Rev. B 57 (1998) 1505–1509.
[21] F. Zhou, K. Kang, T. Maxisch, G. Ceder, D. Morgan, Solid State Commun. 132 (2004) 181–186.
[22] P.E. Blöchl, Phys. Rev. B 50 (1994) 17953–17979.
[23] G. Kresse, D. Joubert, Phys. Rev. B 59 (1999) 1758–1775.
[24] H.J. Monkhorst, J.D. Pack, Phys. Rev. B 13 (1976) 5188–5192.
[25] V.A. Streltsov, E.L. Belokoneva, V.G. Tsirelson, N.K. Hansen, Acta Crystallogr. Sect. B 49 (1993) 147–153.
[26] G. Rousse, J. Rodriguez-Carvajal, S. Patoux, C. Masquelier, Chem. Mater. 15 (2003) 4082–4090.
[27] N.W. Ashcroft, N.D. Mermin, Solid State Physics, Holt, Rinehart and Winston, New York, 1976.
[28] J. Klett, R. Hardy, E. Romine, C. Walls, T. Burchell, Carbon 38 (2000) 953–973.
[29] P.M. Khandare, J.W. Zondlo, A.S. Pavlovic, Carbon 34 (1996) 663–669.
[30] A. Tari, The Specific Heat of Matter at Low Temperatures, Imperial College Press ; Distributed by World Scientific Pub. Co, London: River Edge, NJ, 2003.
[31] C. Delacourt, P. Poizot, J.-M. Tarascon, C. Masquelier, Nat. Mater. 4 (2005) 254–260.
[32] J.L. Dodd, R. Yazami, B. Fultz, Electrochem. Solid-state Lett. 9 (2006) A151–A155.
[33] D. Trefon-Radziejewska, J. Bodzenta, A. Kaźmierczak-Bałata, T. Łukasiewicz, Int. J. Thermophys. 33 (2012) 707–715.
[34] D.D. MacNeil, J.R. Dahn, J. Electrochem. Soc. 148 (2001) A1205–A1210.